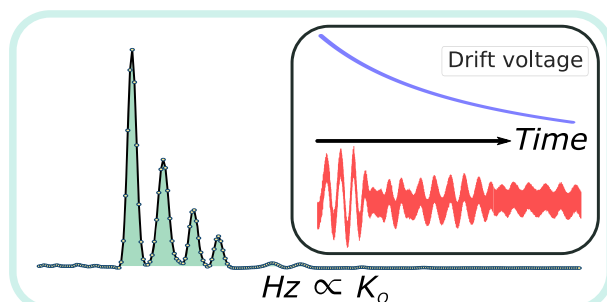


Determination of Gas-Phase Ion Mobility Coefficients Using Voltage Sweep Multiplexing

Tobias Reinecke, Austen L. Davis, Brian H. Clowers 

Department of Chemistry, Washington State University, Pullman, WA 99164, USA



Abstract. In a standard single averaged, drift tube ion mobility spectrometry (IMS) experiment, typically less than 1% of the ions are utilized, with the rest of the ions neutralizing on a closed ion gate or ion optic element. Though some efforts at lower pressures (e.g., 4 Torr) have been made to address this issue by concentrating ions prior to release into a drift cell, the ion current reaching the detector during an IMS experiment is often diminished due to this lower duty cycle. Addition-

ally, when considering the temporal nature of the drift tube IMS experiment and the trajectory of IMS towards higher resolution separations and lower duty cycles, increased detector sampling rates are another factor also which further necessitates new modes of conducting the IMS experiment. Placing this trend in context with ion mobility-mass spectrometry instruments (IM-MS), there are numerous types of mass spectrometers that are simply incompatible with the single averaged ion mobility spectrometry experiments due to timing incompatibilities (i.e., ion traps are an order of magnitude slower than the IMS experiment). However, by utilizing a dual gate ion mobility spectrometer for ion multiplexing, ion utilization efficiency can be significantly increased while creating a measurement signal that can be recorded at low sampling rates. In this work, we present the fundamental theory and first results from proof-of-concept measurements using a new type of ion multiplexing that relies on changing the electric field within the drift cell during the course of an experiment while simultaneously opening the ion gates at a constant frequency. For brevity, this mode is termed voltage sweep multiplexing (VSM). Key variables for this type of experiment are discussed and verified with measurements from traditional signal averaged experiments.

Keywords: Ion mobility spectrometry, Multiplexing, Gas-phase ion separations, Ion mobility fundamentals

Received: 28 November 2018/Revised: 24 February 2019/Accepted: 25 February 2019/Published Online: 15 April 2019

Introduction

In the traditional single gate, single averaged (SGSA) IMS experiment, a small packet of ions is admitted into the drift region of the IMS. Once the ion population crosses the ion gate plane, ion species are separated by their respective drift velocities in a neutral gas under the influence of a weak electric field. At the end of the drift tube, the ions arrive at a detector (commonly a Faraday plate) producing a current or they are transferred to a mass spectrometer (MS) for further analysis. In

recent years, the combination of IMS and MS (IM-MS) has proven to be a very effective analytical tool addressing a range of challenges in the analysis of complex mixtures, including metabolomics [1–3], lipidomics [4], glycomics [5–8], petroleomics [9], and proteomics [10–13]. One major benefit of IM-MS is an increased degree of orthogonality during complex mixtures separation which aids in isotope pattern deconvolution and minimization of chemical noise interferences [14]. Though benefits are realized by the combination of IMS and MS, the hybrid instrument configuration still suffers from diminished levels of ions reaching the detector.

Though efforts have been realized to maximize the level of ions injected into the drift cell (i.e., largely through high pressure ion traps prior to the drift cell) [15–17], the duty cycle of the drift tube IMS experiment remains low with respect to the

Correspondence to: Brian Clowers; e-mail: brian.clowers@wsu.edu

temporal scale of the IM-MS experiment. For example, the ion injection time for a ~ 1 m drift cell coupled to a time of flight mass spectrometer is on the order of 100–400 μs with a total separation time of 100 ms. Under such conditions used to balance resolving power and sensitivity, the duty cycle is 0.1%.

Ion multiplexing is a complementary approach to ion trapping that addresses many of the challenges related to the low duty cycles of the SGSA drift-tube IMS experiments. Previously, we have demonstrated a range of multiplexing techniques including Hadamard [18–21], Fourier [18, 22–24], and correlation-IMS techniques with duty cycles that approach 50% [25]. Especially for mass spectrometry systems (i.e., ion trapping systems) with spectral acquisition rates well below the kilohertz range, multiplexing approaches that use a dual-gate IMS approach represent a viable means to capture mobility information with a reasonable degree of efficiency. Using this instrumental configuration, both Fourier and Hadamard multiplexing are possible [23, 26]. Pseudo-random (e.g., Hadamard) multiplexing using a dual gate system currently requires direct synchronization of the IMS and the ion trapping MS; however, in the case of the Fourier approach, only the start and stop times during the respective domains need be synchronized. In the latter approach, the ion gates are simultaneously opened and closed, while the frequency of opening and closing events is swept linearly. In this way, an interference pattern from the ion current is created, as only ions of certain mobilities can reach the detector for a given frequency. Finally, because the mobility is encoded in the frequency domain, the drift time of an ion population is obtained by directly Fourier-transforming the raw interference pattern and dividing the result by the sweep rate in hertz per second. Using FT-IMS, the duty cycle can be increased from < 1 to 25%. Under select conditions, the duty cycle of the FT-IIMS experiment can be pushed to 50% by emulating the second ion gate using algorithmic approaches [27, 28]. Historically, the pulsing frequency of the dual gate systems is swept over a broad frequency range (e.g., 5–10.005 Hz) in order to minimize peak broadening due to spectral leakage. However, at high frequencies, ion transmission through the gates is significantly diminished known as the gate depletion effect [29].

It is worthy to note that modulation schemes applied to the ion injection element in a drift tube system are not the only approach to enhance experimental duty cycle. Based upon an innovative application of electric fields across a segmented drift cell, overtone mobility spectrometry (OMS) represents a substantially different approach that aims to maximize the efficiency of the ion mobility experiment [30, 31]. Early implementation of OMS relied upon a multigrad structure to realize the mobility filtering approach; however, recent efforts that adopt a radially confining RF field have demonstrated the capacity to realize OMS separation in a gridless system [32]. Using an atmospheric pressure, dual-gate IMS drift cell, we demonstrate a wholly new ion multiplexing method capable of capturing mobility information that also uses time-varying electric fields. Building upon prior voltage sweeping concepts [33, 34], including OMS, in the present proof-of-principle

experiment, the gating frequency of a dual gate IMS is maintained constant, while the applied drift voltage is swept non-linearly. This voltage sweep multiplexing (VSM) experiment yields an ion current interference pattern that directly transforms into the reduced mobility domain instead of the drift time of the ion species. Furthermore, the described multiplexing technique realizes duty cycles of up to 25% while being compatible with comparatively slow detectors. Moreover, because this approach measures ions across a range of electric field strengths, the fundamental theoretical description of the technique suggests the results minimize any errors or experimental bias that would arise from mobility measurements made at a single electric field strength [35–37].

Experimental Methods

VSM experiments were conducted using a PCB-IMS shown in Figure 1 that follows the configuration recently described by Reinecke and Clowers [18]. This system was operated under ambient conditions and temperature (~ 690 Torr and 27°C unless noted otherwise) with a drift region of 10.91 cm. In addition to being constructed out of standard printed circuit board material, this system was equipped with a tri-grid shutter design which obviates the need for a complex Bradbury-Nielsen shutter designs and provides comparatively high levels of performance [38–41]. In close proximity to the Faraday detector, the IMS was equipped with a second, tri-grid ion shutter (see Figure 1) [18, 38].

In order to close the ion gates at the highest electric field strength, a voltage of 80 V was applied to the center grid of the tri-grid ion gate. The floated high voltage pulser electronics were based upon the open-source design previously reported by Garcia et al. [42]. A standard glass capillary (125 μm OD \times 75 μm ID) modified for an electrospray setup was used as an ion source with mixtures being infused at a flow rate of 3 $\mu\text{L}/\text{min}$ using a syringe pump (Fusion 100, Chemyx, Stafford, TX). For the voltage-sweep multiplexing (VSM) experiment, both gates were synchronously opened and closed at a constant frequency using a waveform supplied by a Digilent Analog Discovery unit (Digilent Inc., Pullman, WA). The NIDAQ Tools module extension to IGOR Pro (Lake Oswego, OR) and a NI-6030E Multifunctional DAQ card was used to control the downward sweep of the potentials (Figure 2a) applied to the electrospray source and IMS cell via two Glassman High Voltage FJ-series power supplies. Alternative experimental modes used for comparison were implemented using the same hardware and electronics [22, 23]. Raw spectra were acquired for a series of tetra-alkylammonium salts (TXA) using a Faraday plate, open-source current to voltage amplifier [18], and a Digilent Analog Discovery unit. The specific analytes sourced from Millipore-Sigma (St. Louis, MO) were tetra-pentyl ammonium (T5A) to tetra-octyl ammonium (T8A) and also included tetra-decyl ammonium (T10A) and tetra-dodecyl ammonium (T12A) as either chlorine or bromine salts. Mixtures

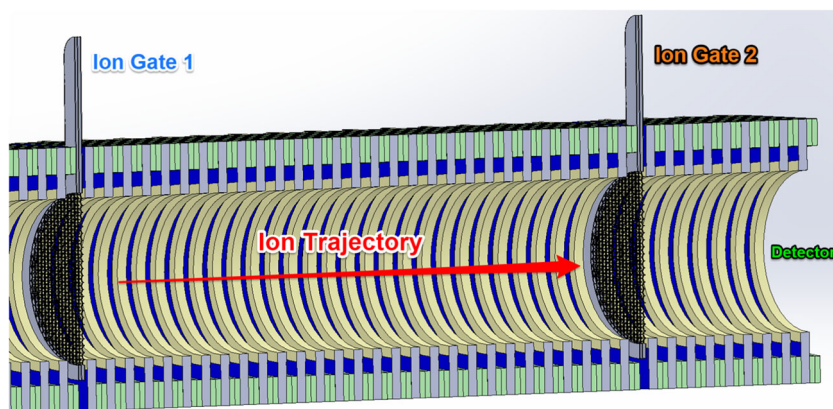


Figure 1. A schematic of the dual-gate PCB-IMS system used. With an ID of 1" and a drift length of 10.91 cm, the optimized geometries combined with PCB manufacturing approach yield a high performance solution to conducting IMS experiments. Ion gating is greatly simplified using a tri-shutter design and etched grids

of these salts were electrosprayed in a 50:50 water:methanol solution at a concentration of $\sim 10 \mu\text{M}$.

Data Processing

Raw interferograms acquired through the VSM approach were processed using a python script following Eqs. (1)–(7). Data were acquired for a single voltage sweep for the specified time

with no signal averaging. To obtain the reduced mobility of the target ion population, the measured frequency, frequency of the ion gating, length of the drift region, and the minimum and maximum voltage were required (Eq. (7)). The measured frequency for each target ion was determined by locating the peak centroid following Fourier transformation and application of a Hamming window. To minimize contributions from the decaying DC component, which originated from the average

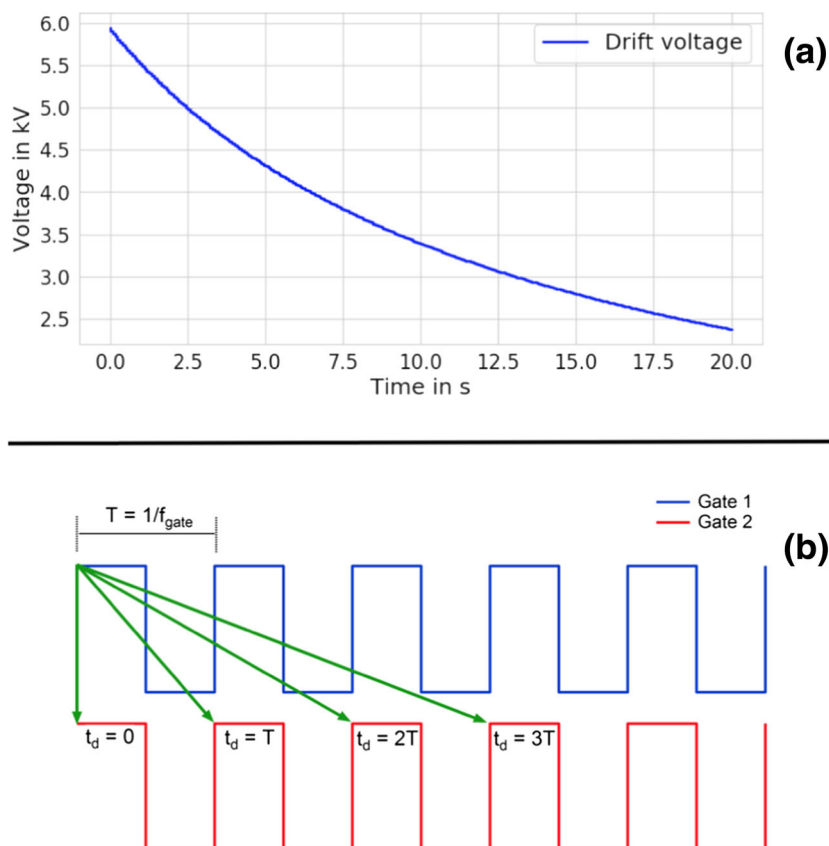


Figure 2. (a) Sweep profile used to perform the described experiments and pulse scheme applied to the respective ion gates (b). The sweep profile was chosen to conform with inverse relation between residence time of an ion in a drift cell and the electric field gradient (see Eq. (1)). Though not shown, the electrospray emitter was held at a constant voltage above the drift voltage to maintain a stable electrospray during the sweep period

ion signal arriving at the detector, a polynomial fit to the raw interferogram was subtracted from the signal prior to Fourier transformation. This data processing step did not alter the peak location but minimized the occurrence of a low frequency offset in the transformed spectra. These procedures were executed for all of the spectra VSM shown.

Theoretical Consideration: Obtaining K_o for Voltage Sweep Multiplexing

Compared to traditional FT-IMS experiments, in the VSM technique, the modulation frequency of both gates is kept constant and the applied drift voltage is swept. Because a change in electric field inside the drift tube results in a change in drift time of the ions, an interference pattern similar to that seen in a traditional FT-IMS (Figure 4a) is observed.

To enhance accuracy of reduced mobility measurements and minimize any biases that may arise from measurements at a single-field setting, drift tube instruments routinely include a series of steps where the electric field strength is varied to construct pressure over voltage (P/U) plots utilizing the independence of mobility from the electric field strength in the low field regime [43, 44]. These experiments are conducted with the express intent to characterize the ion population multiple times at various field strengths and conditions. Subsequently, the mobility of the ions is found from the slope of a linear regression when plotting the observed drift time against $1/U$. As the repetition of measurements for multiple field settings requires an extended amount of time, the present method obviates the need for repeated, independent measurements as the electric field varying is integrated directly into the experiment. At the same time, the Fourier transform of the interference pattern obtained by voltage sweep multiplexing delivers, directly, the mobility coefficient, K , for the ions. Following the description of the theoretical fundamentals, the first results from a proof-of-principle experiment are presented.

As previously stated, during the course of the VSM experiment, both ion gates are simultaneously opened and closed with a constant frequency f_{gate} . Figure 2b depicts the pulsing scheme of both gates. The green arrows illustrate that only ion packets comprised of ions with a drift time equal to a multiple integer n of the gating period T ($t_d = n \times 1/f_{gate} = nT$) will contribute to the signal at the detector, because only then, the complete ion packet traverses the second ion gate during an opening event. On the other hand, ions with a drift time of $t_d = nT/2$ will entirely neutralize on the second ion gate. By definition, the VSM experiment incorporates multiple electric field strengths into single measurements. During the voltage sweep as depicted in Figure 2a, there are multiple, ideal voltage settings where an ion population with a specific mobility will arrive at the detector. Additionally, there is equal number of states in which the same ion packet velocity is destroyed by the ion gate modulation. Combined, these two occurrences yield an interference pattern that contains fundamental ion arrival frequencies that are directly connected to the specific mobility, K , of the ions present.

A concrete path to determining the mobility of the ions from the Fourier transform of the VSM interference pattern can be found by considering the two extreme cases at the beginning (maximum voltage, minimum drift time) and the end (minimum voltage, maximum drift time) of the experiment. The drift time t_d of an ion can be described as

$$t_d = \frac{l}{v_d} = \frac{l^2}{K \cdot U} \quad (1)$$

where, l is the length of the drift region, v_d , the velocity of the ion, K , the mobility of the ion and, U , the applied drift voltage. For a VSM experiment, where the drift voltage is swept downward from U_{max} to U_{min} , the drift time is at a minimum at the beginning of the experiment:

$$t_{d_{min}} = \frac{l^2}{K \cdot U_{max}} \quad (2a)$$

Accordingly, the drift time is at a maximum at the end of the experiment, when the minimum voltage is applied:

$$t_{d_{max}} = \frac{l^2}{K \cdot U_{min}} \quad (2b)$$

In the subsequent step, the minimum and maximum drift time is expressed as a multiple n_{min} and n_{max} of the gate pulse period:

$$t_{d_{min}} = \frac{l^2}{K \cdot U_{max}} = n_{min} \cdot t_{period} = n_{min} \cdot \frac{1}{f_{gate}} \quad (3a)$$

$$t_{d_{max}} = \frac{l^2}{K \cdot U_{min}} = n_{max} \cdot t_{period} = n_{max} \cdot \frac{1}{f_{gate}} \quad (3b)$$

Note that n_{min} and n_{max} are not necessarily integer numbers. Subtracting Eq. (3a from 3b) yields:

$$(n_{max} - n_{min}) \cdot t_{period} = \frac{l^2 \cdot (U_{max} - U_{min})}{K \cdot U_{max} \cdot U_{min}} \quad (4)$$

Consequently, the fundamental frequency observed in the measured interference pattern for a sweep time of t_{sweep} is:

$$f_{meas} = \frac{n_{max} - n_{min}}{t_{sweep}} \quad (5)$$

Combining Eqs. (4) and (5) finally yields the connection between fundamental frequency in a VSM experiment and the mobility of an ion species:

$$f_{meas} \cdot t_{sweep} \cdot \frac{1}{f_{gate}} = \frac{l^2 \cdot (U_{max} - U_{min})}{K \cdot U_{max} \cdot U_{min}} \quad (6)$$

$$K = \frac{1}{f_{meas}} \cdot \frac{f_{gate}}{t_{sweep}} \cdot \frac{l^2 \cdot (U_{max} - U_{min})}{U_{max} \cdot U_{min}} \quad (7)$$

Results and Discussion

Experimental: Proof of Concept for Voltage Sweep IMS Measurements

Using a simple mixture of T5A and T8A as an example, Figure 3b shows the raw spectrum acquired through the VSM experiment. The upper trace in Figure 3a represents the Fourier transform of the raw interferogram acquired over 20 s by ramping the starting voltage from a drift voltage of 5.94 kV down to 2.38 kV all while modulating both gates at 750 Hz. Placing these result in context of the theoretical description (i.e., Eqs. (5)–(7)) illustrates how the beats observed in the raw spectra link to the mobility of the target ions. Close inspection of the interference pattern reveals 17 distinct local maxima which when divided by the sweep time yield the observed frequency for the most intense ion population (i.e., 0.85 Hz). With knowledge of the drift cell length and the minimum and maximum voltage applied, the mobility is readily determined. In this particular case, the reduced mobility for both peaks at 0.846 Hz and 1.156 Hz correspond to $1.094 \text{ cm}^2 \text{ V}^{-1} \text{ s}^{-1}$ and $0.792 \text{ cm}^2 \text{ V}^{-1} \text{ s}^{-1}$ which are in reasonable agreement with literature reports for T5A and T8A, respectively [45].

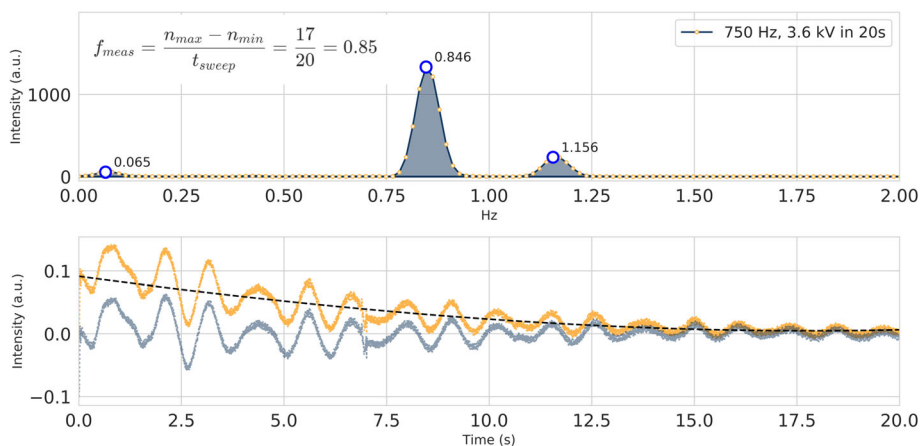


Figure 3. (a) Transformed VS-IMS result from the data in (b). As an illustrative exercise, counting the number of beats observed divided by the sweep time yields the observed frequency. The relationship between this value and the mobility is derived in the theoretical section

Comparison to Traditional Multiplexing Approaches: FT-IMS

To assess the analytical performance of the dual gate IMS system and establish a baseline for comparison, a traditional Fourier transform–ion mobility spectrometry (FT-IMS) experiment was performed prior to the VSM experiment. Here, the applied voltage was kept constant (545 V/cm) and both ion gates were opened and closed simultaneously with a linearly increasing frequency in a range of $f=5 \text{ Hz}$ to $f=10.005 \text{ kHz}$ over the course of 10 s.

Figure 4a depicts the interference pattern of the ion current measured at the Faraday detector for the FT-IMS experiment. Focusing on the downward trend of the interferogram, the ion-gate depletion effect is clearly visible, as the ion current significantly decreases towards higher measurement times (i.e., higher gating frequencies). As shown in Figure 4a and b, Fourier-transforming the interference pattern yields a set of peaks whose location, when divided by the gate modulation sweep rate, yields the drift time spectrum commonly found in a SGSA experiment. The peaks observed in Figure 4 corresponded to a series of tetralkylammonium salts (T5A, T6A, T7A, T8A, T10A, and T12A). For the VSM result shown in Figure 4c, the polynomial-corrected interference pattern was transformed into the frequency domain with the more traditional spectrum shown in Figure 4d. The maximum resolving power for the FT-IMS experiment was ~ 75 , while for the VSM experiment the resolving power reached 30. Though lower than the traditional approach by more than a factor of 2, the VSM results in a spectrum with nominally the same relative peak heights and locations. Moreover, the resolution attained in the FT-IMS experiment is directly linked to the highest gating frequency gating cycle which, unfortunately, often corresponds to the highest degree of gate depletion. In the VSM experiment, the experimental resolving power is limited by the number of data points collected and the “ion beats” (i.e., oscillations in the interference pattern) at the detector. For the conditions examined, no signal averaging was

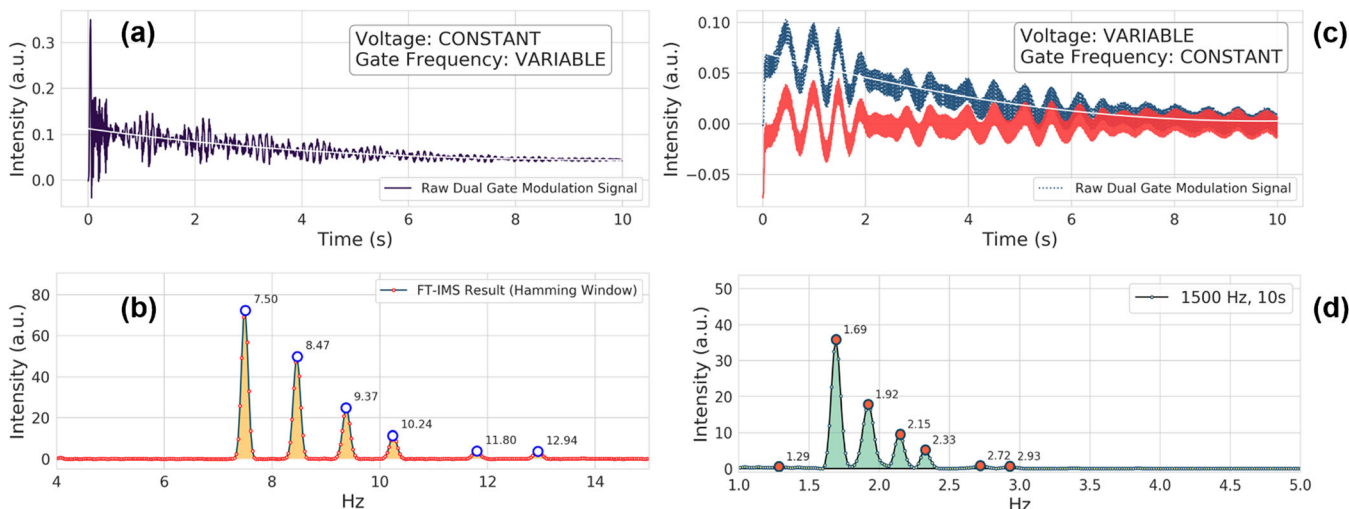


Figure 4. (a) Raw FT-IMS signal for the TXA mixture. With the voltage gradient held constant, the frequency was swept from 5 to 10.005 Hz in 10 s. (b) Transformed results from the traditional FT-IMS data. The resolving power, R_p , defined as drift time t_d divided by the peak width at half maximum for the data shown in (b) was approximately 75. (c) Raw data from a single voltage sweep experiment with a sweep potential across 3.56 kV in 10 s. The raw data were corrected for the signal decay induced by lower ion signal at decreased field strengths. (d) Fourier-transformed result of the raw data along with the observed frequencies of the TXA salts present (T5-8A, T10A, and T12A)

performed, nor was the sweeping cycle repeated. Using these approaches, the resolving power of the VSM experiment may be pushed to levels that may exceed the FT-IMS experiment.

Optimization of VSM Results

To highlight more clearly, the impact on ion gating frequency, a subsequent set of experiments across a broader frequency range, was conducted. As can be seen from Eqs. (6) and (7), the parameters that need be adjusted in order to perform a VSM experiment are the sweep time, t_{sweep} , gating frequency, f_{gate} , and the voltage sweep range based on U_{max} and U_{min} . Before determining the sweep time, the voltage range and gating frequency need to be set. For an ideal system, theory predicts higher resolving powers for higher gating frequencies and broader voltage sweep range, as this leads to a larger number of oscillations in the interference pattern (i.e., higher value for $(n_{\text{max}} - n_{\text{min}})$) and thus less peak broadening due to spectral leakage in the Fourier transform. In a real system, however, the maximum achievable number of oscillations in the interference pattern is limited by different factors, requiring a balance between gating frequency and voltage sweep range. The maximum voltage is simply limited by the breakdown voltage of the system while the maximum gating frequency and minimum voltage are predominantly determined by the gate depletion effect [29, 46]. The gate depletion effect arises from the fact that an ion packet requires a certain time to pass through the gate. Therefore, excessively high gating frequencies restrain the ion packet from reaching the detector and producing a measurable signal. Similarly, overly low voltages cause a low velocity of the ion packet, which increases the impact of gate depletion and also lead to significant deterioration of the ion current, even at low gating frequencies. Combining all of these

factors with the additional diffusion contributions to peak broadening, the present section focused on identifying optimum settings through experimental means. When considering the VSM experiment, it is important to note that the drift time of an ion is inversely proportional to the applied drift voltage. Though obvious in hindsight, initial experiments using a linear sweep produced results that could not be linked to theory precisely because this point was overlooked. Consequently, it is crucial for VSM that the voltage sweep profile be inversely proportional (see Figure 2a) to the sweep time in order to realize a linear sweep of the ions' drift time.

For the apparatus used, the maximum voltage that could be applied to the first ring of the desolvation region was 12.5 kV, leading to a voltage of 6.78 kV applied to the first gate and 0.84 kV second gate respectively. This leads to a maximum drift voltage of $U_{\text{max}} = 5.94$ kV. At a minimum voltage of 5 kV applied to the first ring, the potential on the first gate was 2.72 kV and 0.34 kV on the second gate leading to a minimum drift voltage $U_{\text{min}} = 2.38$ kV. Based on these settings, the expected fundamental frequency in the interference pattern f_{meas} for ions with different mobilities K can be calculated in dependency of the sweep time t_{meas} using Eq. (7). Then, the minimum sweep time (i.e., minimum measurement time) is mainly determined by the Nyquist theorem which dictates the sampling rate of the employed detector. The Nyquist theorem states that a signal needs to be sampled with a sampling rate of at least $f_{\text{sampling}} = 2 f_{\text{meas}}$ in order to be exactly reconstructed. When using a detector with a high sampling rate, another limiting factor in terms of reducing the sweep time could be parasitic capacitance of the drift tube when the sweep time is in the same range as the time constant of the setup. In this case, the applied voltage and the actual voltage on the IMS might diverge introducing distortions in the measurement signal.

Therefore, t_{sweep} was set to 20 s for these initial experiments, even though the sampling rate of 100 kS/s provided by the Digilent Analog Discovery would allow faster sweeps.

When choosing a gating frequency for the experiment, there are two main factors that need to be considered. According to Eq. (7), higher gating frequencies lead to higher frequencies observed in the measured raw data. A higher measurement frequency implies more oscillations in the measurement signal resulting in increased resolution after Fourier-transforming the data. However, higher gating frequencies also imply that the gate is opened for a shorter time which in term leads to an increased gate depletion effect, especially for low voltage settings where the ions are moving at reduced velocity. When ion transmission through the gates is significantly decreased due to gate depletion effect, the oscillation in ion current might not be measurable, resulting in peak broadening and low signal to noise ratio.

In order to investigate the influence of the gating frequency, VSM data for a mixture containing T5A and T8A were collected. The reported literature values for the reduced mobilities in nitrogen are $K_{o,\text{TX5}} = 1.116 \text{ cm}^2 \text{ V}^{-1} \text{ s}^{-1}$ and $K_{o,\text{TX8}} = 0.808 \text{ cm}^2 \text{ V}^{-1} \text{ s}^{-1}$ [47]. Independent verification of the reduced mobility values in our laboratory with a standalone ion mobility spectrometer in SGSA mode yielded $K_{o,\text{TX5}} = 1.073 \text{ cm}^2 \text{ V}^{-1} \text{ s}^{-1}$ and $K_{o,\text{TX8}} = 0.782 \text{ cm}^2 \text{ V}^{-1} \text{ s}^{-1}$. As mentioned in the

experimental section, in order to remove DC and low frequency components from the signal, a polynomial is fitted to the mean of the raw data and subsequently subtracted. Furthermore, a Hanning window was applied for side lobe reduction. The drift gas for all presented experiments is nitrogen with flow rate of 500 mL/min. For this set of experiments, the temperature in the laboratory was $T = 293 \text{ K}$ and the pressure was $P = 695 \text{ Torr}$.

Figure 5a shows the results from a voltage sweep with $f_{\text{gate}} = 500 \text{ Hz}$ gating frequency. Even though there are only two analyte ions in the sample, four peaks are detected in the transformed spectrum. The first peak at a frequency of $f_{\text{meas}} = 0.081 \text{ Hz}$ is attributed to a residual low frequency component that could not be removed with the polynomial fitting procedure. Further peaks in the spectrum appear at a frequency of $f_{\text{meas}} = 0.326 \text{ Hz}$ which, according to Eq. (7) corresponds to a reduced mobility of $K_o = 1.957 \text{ cm}^2 \text{ V}^{-1} \text{ s}^{-1}$ which was attributed to a solvent peak. The peak in Figure 5a $f_{\text{meas}} = 0.553 \text{ Hz}$ with a corresponding $K_o = 1.154 \text{ cm}^2 \text{ V}^{-1} \text{ s}^{-1}$ and $f_{\text{meas}} = 0.814 \text{ Hz}$ with $K_o = 0.784 \text{ cm}^2 \text{ V}^{-1} \text{ s}^{-1}$. Comparing the K_o values to the literature values reveals that the actual analyte peaks are the peaks at $f_{\text{meas}} = 0.553 \text{ Hz}$ and $f_{\text{meas}} = 0.814 \text{ Hz}$. The obtained mobility spectrum apparently suffers from reduced accuracy which is mainly attributed to the low gating frequency. Therefore, the gating frequency was increased to $f_{\text{gate}} = 750 \text{ Hz}$ in the next step.

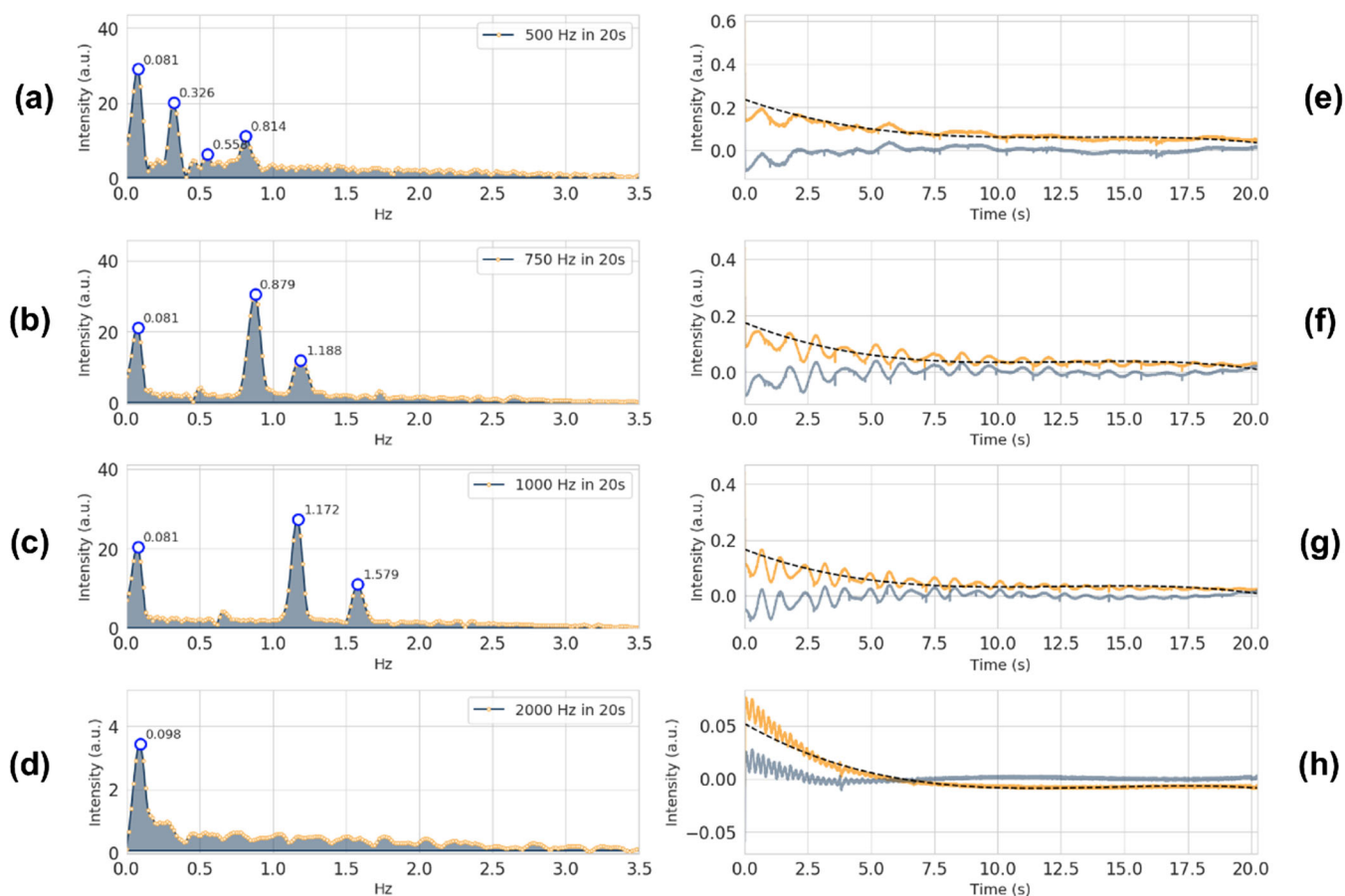


Figure 5. Transformed VMS results (left-hand column) from the raw data (right-hand column) for a VSM experiment and different gating frequencies. These data illustrate the impact of gate-depletion and choice of gating frequency on the observed VSM result

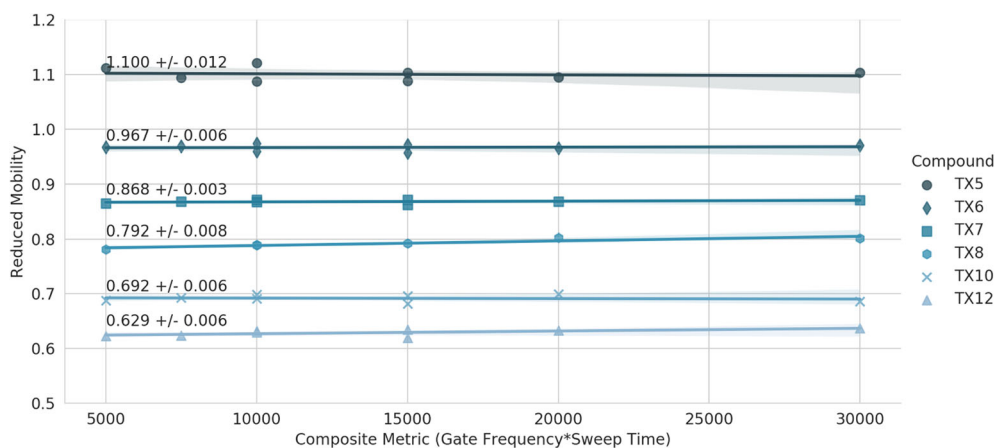


Figure 6. Across a range of experimental conditions, the reduced mobilities from the voltage sweep method are within 2% of previously reported values in nitrogen at room temperature. The units for the reported values are $\text{cm}^2 \text{V}^{-1} \text{s}^{-1}$

As predicted by theory, the analyte peaks in Figure 5b are found at higher frequencies compared to the measurement at a lower gating frequency (Figure 5a). Both analyte peaks are clearly separated and found at $f_{\text{meas}} = 0.879 \text{ Hz}$ with a corresponding $K_0 = 1.074 \text{ cm}^2 \text{V}^{-1} \text{s}^{-1}$ and $f_{\text{meas}} = 1.188 \text{ Hz}$ with a corresponding $K_0 = 0.795 \text{ cm}^2 \text{V}^{-1} \text{s}^{-1}$. The resolving powers defined as the peak centroid divided by the peak width at half-maximum were $R_{\text{T5A}} = 10$ for the T5A peak and $R_{\text{T8A}} = 11$ for the T8A peak. Increasing the resolving power is possible by further increasing the frequency to $f_{\text{gate}} = 1000 \text{ Hz}$ (Figure 5c) reducing peak broadening largely due to a reduction in spectral leakage [48]. Again, two clearly separated peaks are visible at $f_{\text{meas}} = 1.172 \text{ Hz}$ and $f_{\text{meas}} = 1.579 \text{ Hz}$ with corresponding reduced mobility values of $K_0 = 1.089 \text{ cm}^2 \text{V}^{-1} \text{s}^{-1}$ and $K_0 = 0.808 \text{ cm}^2 \text{V}^{-1} \text{s}^{-1}$ respectively. As predicted, the resolving power increases to $R_{\text{T5A}} = 14$ and $R_{\text{T8A}} = 19$. Though further increasing the gating frequency to $f_{\text{gate}} = 2000 \text{ Hz}$ results in a rapid oscillations in the raw data, there was also a significant decay in ion current at lower electric field strengths (Figure 5h). This rapid decay, not surprisingly, does not lead to a sufficient number of oscillations for faithful transformation (Figure 5d).

From these sets of experiments, it can be seen that the gating frequency has a major impact on the quality of the transformed VSM spectrum. Higher gating frequencies are desirable as they lead to a better resolution of the peaks in the spectrum because broadening due to spectral leakage decreases with higher measurement frequencies. However, with the current instrumental configuration, ion loss caused by the gate depletion effect prevents successful measurements at high gating frequencies. For choosing the optimum frequency across a given voltage sweep range, a rough knowledge of the target analyte mobility is necessary as the gate depletion effect critically depends on the velocity of the ions traversing the ion gate. This parameter may be readily estimated by leveraging the loose relationship between mass and mobility which can be used to constrain the range of possible optimum target frequencies. An option for significantly improving the setup could be a recently published type of ion shutter that showed promising results for minimizing gate depletion effect [46]. Not only could this lead to

improved results for higher gating frequencies, also increasing the chirp range towards lower voltages seems feasible with this approach.

Determination of Reduced Mobility Values Using VSM

Using the same mixture shown in Figure 4, a range of different conditions were explored to evaluate their impact on the measured ion mobilities. Specifically, experiments using all combinations for two different sweep times (i.e., 10 and 20 s) and four different ion gate modulation frequencies (i.e., 500, 750, 1000, and 1500 Hz) were conducted. Figure 6 shows the observed mobilities derived from the VSM experiments across the range of conditions examined. The x-axis is a composite metric of the gating frequency and the sweep time used which simply aids in display of the data. Included in this plot are confident bands associated with each individual ion set along with annotated values for each of the ions. These experiments illustrate a high degree of precision with reduced mobility values for all of the TXA salts examined varying by less than 0.1% on average. Compared to literature values reported from a lower pressure instrument (i.e., 4 Torr), the results were within 2%. When factoring in the instrument specifics of the apparatus used in the literature and potential issues with field matching in ion funnels [44, 45], these results highlight the capacity of the VSM experiment to produce mobility values using a wholly different approach.

Conclusion

A new class of ion multiplexing was described both theoretically and experimentally that integrates mobility measurements across different electric field strengths with a dual gate IMS. This voltage sweep multiplexing provides a high degree of ion utilization efficiency while being compatible to slow acquisition mass detectors. In addition to demonstrating a high degree of agreement between mobility values obtained using VSM, the potential exists to extend the resolving power of the

technique by integrating multiple voltage sweeps during a single experiment and coupling the system with a mass analyzer. The latter will surely prove beneficial as the interference pattern for a single m/z may be selected and transformed. Current IM-MS platforms that use only a single gate may be compatible with the VSM technique simply by modulating an ion optic element closer to the detector. Though the resolving power for the VSM result was lower than some of the traditional means, it represents a new experimental mode that may serve as a validating experiment due to the range of electric fields probed in a single experiment. Future efforts will focus on coupling a VSM-compatible drift cell to a mass analyzer and developing a quantitative accounting of diffusion during the VSM experiment. A full accounting of ion packet evolution during the experiment may provide a means to vary both frequency and the electric field simultaneously to realize a fully optimized multiplexing experiment.

Acknowledgements

TR and ALD were supported in part by the DTRA Basic Research Program (HDTRA1-14-1-0023). Additional support was provided through the National Science Foundation (CHE-1506672).

References

- Paglia, G., Williams, J.P., Menikarachchi, L., Thompson, J.W., Tyldesley-Worster, R., Halldórsson, S., Rolfsson, O., Moseley, A., Grant, D., Langridge, J., Palsson, B.O., Astarita, G.: Ion mobility derived collision cross sections to support metabolomics applications. *Anal. Chem.* **86**, 3985–3993 (2014)
- Dwivedi, P., Wu, P., Klopsch, S.J., Puzon, G.J., Xun, L., Hill, H.H.: Metabolic profiling by ion mobility mass spectrometry (IMMS). *Metabolomics*. **4**, 63–80 (2007)
- Dear, G.J., Munoz-Muriedas, J., Beaumont, C., Roberts, A., Kirk, J., Williams, J.P., Campuzano, I.: Sites of metabolic substitution: investigating metabolite structures utilising ion mobility and molecular modelling. *Rapid Commun. Mass Spectrom.* **24**, 3157–3162 (2010)
- Kliman, M., May, J.C., McLean, J.A.: Lipid analysis and lipidomics by structurally selective ion mobility-mass spectrometry. *Biochim. Biophys. Acta.* **1811**, 935–945 (2011)
- Morrison, K.A., Clowers, B.H.: Contemporary glycomic approaches using ion mobility-mass spectrometry. *Curr. Opin. Chem. Biol.* **42**, 119–129 (2018)
- Nagy, G., Attah, I.K., Garimella, S.V.B., Tang, K., Ibrahim, Y.M., Baker, E.S., Smith, R.D.: Unraveling the isomeric heterogeneity of glycans: ion mobility separations in structures for lossless ion manipulations. *Chem. Commun.* **54**, 11701–11704 (2018)
- Zheng, X., Zhang, X., Schocker, N.S., Renslow, R.S., Orton, D.J., Khamsi, J., Ashmus, R.A., Almeida, I.C., Tang, K., Costello, C.E., Smith, R.D., Michael, K., Baker, E.S.: Enhancing glycan isomer separations with metal ions and positive and negative polarity ion mobility spectrometry-mass spectrometry analyses. *Anal. Bioanal. Chem.* **409**, 467–476 (2017)
- Huang, Y., Dodds, E.D.: Ion mobility studies of carbohydrates as group I adducts: isomer specific collisional cross section dependence on metal ion radius. *Anal. Chem.* **85**, 9728–9735 (2013)
- Fasciotti, M., Lalli, P.M., Klitzke, C.F., Corilo, Y.E., Pudenz, M.A., Pereira, R.C.L., Bastos, W., Daroda, R.J., Eberlin, M.N.: Petroleomics by traveling wave ion mobility-mass spectrometry using CO₂ as a drift gas. *Energy Fuel.* **27**, 7277–7286 (2013)
- Valentine, S.J., Plasencia, M.D., Liu, X., Krishnan, M., Naylor, S., Udseth, H.R., Smith, R.D., Clemmer, D.E.: Toward plasma proteome profiling with ion mobility-mass spectrometry. *J. Proteome Res.* **5**, 2977–2984 (2006)
- Helm, D., Vissers, J.P.C., Hughes, C.J., Hahne, H., Ruprecht, B., Pachi, F., Grzyb, A., Richardson, K., Wildgoose, J., Maier, S.K., Marx, H., Wilhelm, M., Becher, I., Lemeer, S., Bantscheff, M., Langridge, J.I., Kuster, B.: Ion mobility tandem mass spectrometry enhances performance of bottom-up proteomics. *Mol. Cell. Proteomics.* **13**, 3709–3715 (2014)
- Crowell, K.L., Slys, G.W., Baker, E.S., LaMarche, B.L., Monroe, M.E., Ibrahim, Y.M., Payne, S.H., Anderson, G.A., Smith, R.D.: LC-IMS-MS feature finder: detecting multidimensional liquid chromatography, ion mobility and mass spectrometry features in complex datasets. *Bioinformatics.* **29**, 2804–2805 (2013)
- Burnum-Johnson, K.E., Nie, S., Casey, C.P., Monroe, M.E., Orton, D.J., Ibrahim, Y.M., Gritsenko, M.A., Clauss, T.R.W., Shukla, A.K., Moore, R.J., Purvine, S.O., Shi, T., Qian, W., Liu, T., Baker, E.S., Smith, R.D.: Simultaneous proteomic discovery and targeted monitoring using liquid chromatography, ion mobility spectrometry, and mass spectrometry. *Mol. Cell. Proteomics.* **15**, 3694–3705 (2016)
- May, J.C., McLean, J.A.: Ion mobility-mass spectrometry: time-dispersive instrumentation. *Anal. Chem.* **87**, 1422–1436 (2015)
- Clowers, B.H., Ibrahim, Y.M., Prior, D.C., Danielson, W.F., Belov, M.E., Smith, R.D.: Enhanced ion utilization efficiency using an electrodynamic ion funnel trap as an injection mechanism for ion mobility spectrometry. *Anal. Chem.* **80**, 612–623 (2008)
- Ibrahim, Y.M., Garimella, S.V.B., Tolmachev, A.V., Baker, E.S., Smith, R.D.: Improving ion mobility measurement sensitivity by utilizing helium in an ion funnel trap. *Anal. Chem.* **86**, 5295–5299 (2014)
- Hoaglund, C.S., Valentine, S.J., Clemmer, D.E.: An ion trap interface for ESI-ion mobility experiments. *Anal. Chem.* **69**, 4156–4161 (1997)
- Reinecke, T., Clowers, B.H.: Implementation of a flexible, open-source platform for ion mobility spectrometry. *HardwareX.* **4**, e00030 (2018)
- Clowers, B.H., Siems, W.F., Hill, H.H., Massick, S.M.: Hadamard transform ion mobility spectrometry. *Anal. Chem.* **78**, 44–51 (2006)
- Clowers, B.H., Belov, M.E., Prior, D.C., Danielson 3rd, W.F., Ibrahim, Y., Smith, R.D.: Pseudorandom sequence modifications for ion mobility orthogonal time-of-flight mass spectrometry. *Anal. Chem.* **80**, 2464–2473 (2008)
- Szumlas, A.W., Ray, S.J., Hieftje, G.M.: Hadamard transform ion mobility spectrometry. *Anal. Chem.* **78**, 4474–4481 (2006)
- Knorr, F.J., Eatherton, R.L., Siems, W.F., Hill Jr., H.H.: Fourier transform ion mobility spectrometry. *Anal. Chem.* **57**, 402–406 (1985)
- Morrison, K.A., Siems, W.F., Clowers, B.H.: Augmenting ion trap mass spectrometers using a frequency modulated drift tube ion mobility spectrometer. *Anal. Chem.* **88**, 3121–3129 (2016)
- Poltash, M.L., McCabe, J.W., Shirzadeh, M., Laganowsky, A., Clowers, B.H., Russell, D.H.: Fourier transform-ion mobility-Orbitrap mass spectrometer: a next-generation instrument for native mass spectrometry. *Anal. Chem.* **90**, 10472–10478 (2018)
- Davis, A.L., Liu, W., Siems, W.F., Clowers, B.H.: Correlation ion mobility spectrometry. *Analyst.* **142**, 292–301 (2017)
- Tummalacherla, M., Garimella, S.V.B., Prost, S.A., Ibrahim, Y.M.: Toward artifact-free data in Hadamard transform-based double multiplexing of ion mobility-Orbitrap mass spectrometry. *Analyst.* **142**, 1735–1745 (2017)
- Tarver, E.E.: External second gate Fourier transform ion mobility spectrometry: parametric optimization for detection of weapons of mass destruction. In: IEEE 37th Annual 2003 International Carnahan Conference on Security Technology, 2003. Proceedings
- Tarver, E.: External second gate, Fourier transform ion mobility spectrometry: parametric optimization for detection of weapons of mass destruction. *Sensors.* **4**, 1–13 (2004)
- Puton, J., Knap, A., Siodłowski, B.: Modelling of penetration of ions through a shutter grid in ion mobility spectrometers. *Sens. Actuators B Chem.* **135**, 116–121 (2008)
- Kurulugama, R.T., Nachtigall, F.M., Lee, S., Valentine, S.J., Clemmer, D.E.: Overtone mobility spectrometry: part 1. Experimental observations. *J. Am. Soc. Mass Spectrom.* **20**, 729–737 (2009)
- Valentine, S.J., Stokes, S.T., Kurulugama, R.T., Nachtigall, F.M., Clemmer, D.E.: Overtone mobility spectrometry: part 2. Theoretical considerations of resolving power. *J. Am. Soc. Mass Spectrom.* **20**, 738–750 (2009)
- Zucker, S.M., Ewing, M.A., Clemmer, D.E.: Gridless overtone mobility spectrometry. *Anal. Chem.* **85**, 10174–10179 (2013)

33. Davis, E.J., Clowers, B.H., Siems, W.F., Hill, H.H.: Comprehensive software suite for the operation, maintenance, and evaluation of an ion mobility spectrometer. *Int. J. Ion Mobil. Spec.* **14**, 117 (2011)
34. Davis, E.J., Williams, M.D., Siems, W.F., Hill Jr., H.H.: Voltage sweep ion mobility spectrometry. *Anal. Chem.* **83**, 1260–1267 (2011)
35. Davis, A.L., Clowers, B.H.: Leveraging spectral sparsity to realize enhanced separation of gas-phase ion populations. *Int. J. Mass Spectrom.* **427**, 141–150 (2018)
36. Hauck, B.C., Siems, W.F., Harden, C.S., McHugh, V.M., Hill Jr., H.H.: Determination of E/N influence on K values within the low field region of ion mobility spectrometry. *J. Phys. Chem. A.* **121**, 2274–2281 (2017)
37. Wyttenbach, T., Bowers, M.T.: Gas-phase conformations: the ion mobility/ion chromatography method. In: *Topics in Current Chemistry*. pp. 207–232 (2003)
38. Langejuergen, J., Allers, M., Oermann, J., Kirk, A., Zimmermann, S.: High kinetic energy ion mobility spectrometer: quantitative analysis of gas mixtures with ion mobility spectrometry. *Anal. Chem.* **86**, 7023–7032 (2014)
39. Du, Y., Cang, H., Wang, W., Han, F., Chen, C., Li, L., Hou, K., Li, H.: Note: design and construction of a simple and reliable printed circuit board-substrate Bradbury-Nielsen gate for ion mobility spectrometry. *Rev. Sci. Instrum.* **82**, 086103 (2011)
40. Yoon, O.K., Zuleta, I.A., Robbins, M.D., Barbula, G.K., Zare, R.N.: Simple template-based method to produce Bradbury-Nielsen gates. *J. Am. Soc. Mass Spectrom.* **18**, 1901–1908 (2007)
41. Kai, N., Jingran, G., Guangli, O., Yu, L., Quan, Y., Xiang, Q., Xiaohao, W.: A simple template-based transfer method to fabricate Bradbury-Nielsen gates with uniform tension for ion mobility spectrometry. *Rev. Sci. Instrum.* **85**, 085107 (2014)
42. Garcia, L., Saba, C., Manocchio, G., Anderson, G.A., Davis, E., Clowers, B.H.: An open source ion gate pulser for ion mobility spectrometry. *Int. J. Ion Mobil. Spectrom.* **20**, 87–93 (2017)
43. Siems, W.F., Viehland, L.A., Hill Jr., H.H.: Improved momentum-transfer theory for ion mobility. 1. Derivation of the fundamental equation. *Anal. Chem.* **84**, 9782–9791 (2012)
44. Baker, E.S., Clowers, B.H., Li, F., Tang, K., Tolmachev, A.V., Prior, D.C., Belov, M.E., Smith, R.D.: Ion mobility spectrometry-mass spectrometry performance using electrodynamic ion funnels and elevated drift gas pressures. *J. Am. Soc. Mass Spectrom.* **18**, 1176–1187 (2007)
45. May, J.C., Morris, C.B., McLean, J.A.: Ion mobility collision cross section compendium. *Anal. Chem.* **89**, 1032–1044 (2017)
46. Kirk, A.T., Grube, D., Kobelt, T., Wendt, C., Zimmermann, S.: High-resolution high kinetic energy ion mobility spectrometer based on a low-discrimination tristate ion shutter. *Anal. Chem.* **90**, 5603–5611 (2018)
47. May, J.C., Goodwin, C.R., Lareau, N.M., Leaprot, K.L., Morris, C.B., Kurulugama, R.T., Mordehai, A., Klein, C., Barry, W., Darland, E., Overney, G., Imatani, K., Stafford, G.C., Fjeldsted, J.C., McLean, J.A.: Conformational ordering of biomolecules in the gas phase: nitrogen collision cross sections measured on a prototype high resolution drift tube ion mobility-mass spectrometer. *Anal. Chem.* **86**, 2107–2116 (2014)
48. Qian, W., Xiao, Y., Yong, R.: Spectrum leakage suppression for multi-frequency signal based on DFT. In: *2017 13th IEEE International Conference on Electronic Measurement & Instruments (ICEMI)*. Pp. 394–399. IEEE (2017)